



Radioiodinated sunitinib as a potential radiotracer for imaging angiogenesis—radiosynthesis and first radiopharmacological evaluation of 5- ^{125}I]Iodo-sunitinib

Manuela Kuchar^a, Maria Cristina Oliveira^b, Lurdes Gano^b, Isabel Santos^b, Torsten Knies^{a,*}

^a Institute of Radiopharmacy, Helmholtz-Zentrum Dresden-Rossendorf e.V., POB 510119, D-01314 Dresden, Germany

^b Unidade de Ciências Químicas e Radiofarmacêuticas, Instituto Tecnológico e Nuclear, Estrada Nacional 10, 2686-953 Sacavém, Portugal

ARTICLE INFO

Article history:

Received 20 January 2012

Revised 21 February 2012

Accepted 22 February 2012

Available online 1 March 2012

Keywords:

Sunitinib[®]

VEGFR

RTKs

Iodine-125

Radiolabeling

ABSTRACT

Sunitinib[®] (SU11248) is a highly potent tyrosine kinase inhibitor targeting vascular endothelial growth factor receptor (VEGFR). Radiolabeled inhibitors of RTKs might be useful tools for monitoring RTKs levels in tumour tissue giving valuable information for anti-angiogenic therapy. We report here the synthesis of a ^{125}I -labeled derivative of sunitinib[®] and its first radiopharmaceutical characterization.

The non-radioactive reference compound 5-iodo-sunitinib **4** was prepared by Knoevenagel condensation of 5-iodo-oxindole with the corresponding substituted 5-formyl-1H-pyrrole. In a competition binding assay against VEGFR-2 a binding constant (K_d) of 16 nM for **4** was found. The ability of **4** to inhibit tyrosine kinase activity was demonstrated on RTK expressing cells suggesting this radiotracer as a useful tool for monitoring VEGFR expression. 5- ^{125}I]Iodo-sunitinib, [^{125}I]-**4** was obtained via destannylation of the corresponding tributylstannyl precursor with [^{125}I]NaI in the presence of H_2O_2 in high radiochemical yield (>95%) and radiochemical purity (<98%) after HPLC purification. Determination of human plasma protein binding at time intervals of 0; 1; 2; 4 and 24 h suggested a low non-specific binding of 5–10%. Preliminary biodistribution studies of [^{125}I]-**4** in healthy CD-1 mice showed a relatively high uptake in VEGFR-2 rich tissues like kidney and lung followed by rapid washout (9.6 and 9.7; 4.5 and 3.8% ID/g of kidney and lung at 1 and 4 h, respectively).

© 2012 Elsevier Ltd. All rights reserved.

The vascular endothelial growth factor (VEGF) and platelet-derived growth factor (PDGF) have been well validated targets for treatment of cancer due to their important roles in the growth and nutrition of tumours. The receptor tyrosine kinases (RTKs) of both growth factors have been found to be overexpressed in melanoma and glioma cells and by participating in the transmission of signals for proliferation, migration and differentiation between tumour and endothelial cells and they are considered as master switches in tumour angiogenesis.¹

The increasing number of targeted tumor therapies includes treatment with inhibitors of RTKs and is accompanied with a more sensitive need for dose optimization and monitoring therapeutic response. Direct non-invasive molecular imaging of tumour vascularization and angiogenic processes in vitro would facilitate the selection of patients and help to evaluate the efficacy of anti-angiogenic therapies.^{2–4} Radionuclide-based imaging technologies, like PET and SPECT, are progressively affecting the clinical diagnosis and treatment of cancer. A reliable and accurate in vivo quantitative method to determine the levels of VEGFR-expression would

help to develop a customized VEGFR-targeted cancer therapy. Consequently small molecule RTK inhibitors have been radiolabeled with positron emitters (fluorine-18, carbon-11) and SPECT radioisotopes (technetium-99m, iodine-123) as radioactive probes for imaging RTK expression.⁵ Recent efforts employing the 4-anilinoquinazoline scaffold (characteristic of EGFR tyrosine kinase inhibitors) included the development of ^{11}C -PAQ.⁶ Immunohistochemical analysis of receptor expression in different xenograft models has indicated that the radiotracer uptake in tumour correlated well with variations in the VEGFR-2 expression. Other ^{11}C -labeled compounds for this target, based upon an indole-maleimide core have been published. However in spite of the encouraging in vitro results, the radiolabeled lead tracer failed to accumulate in VEGFR-2 overexpressing tumors.⁷ Dual receptor probes for VEGF/PDGF tyrosine kinase, radiolabeled with carbon-11 or fluorine-18 were prepared as well, but the evaluation of their potential as PET angiogenic probes is still underway.^{8,9} Similarly to radiotracers developed for EGFR tyrosine kinase^{10–13}, radiotracers targeting VEGFR tyrosine kinase have not proved yet to be useful for clinical applications despite promising in vitro evaluations and systematic studies to determine optimal properties for imaging this target are still warranted.⁵

* Corresponding author. Tel.: +49 351 260 2760; fax: +49 351 260 2915.

E-mail address: t.kniess@hzdr.de (T. Knies).

Small molecule tyrosine kinase inhibitors based on the indoline-2-one type like semaxanib[®] (SU5416), TSU68[®] (SU6668) and sunitinib[®] (SU11248) have shown high inhibition values for VEGFR and PDGFR or both (Scheme 1). The 5-fluoro-substituted derivative sunitinib[®] was approved in 2006 as a chemotherapeutic drug for treatment of renal cell carcinoma (RCC) and gastrointestinal stromal tumours (GIST).

Efforts to design radiolabeled VEGFR RTK inhibitors also pursued the radiolabeling of known inhibitors or their analogues. For example, the radiosynthesis of ¹⁸F-sunitinib by radiofluorination of the corresponding nitro-precursor has been described, however, as far as we know no radiopharmacological data were provided up to now.¹⁴ We have contributed to this topic by the development of the fluorine-18 radiolabeled VEGFR inhibitor ¹⁸F-SU5205 as a possible radiotracer for imaging VEGFR-RTKs, but the tracer failed to show a specific uptake in tumors.¹⁵

Our aim with ongoing studies was to focus on the oxindole structure of sunitinib[®] owing to its high cellular activity against VEGF and PDGF (IC₅₀ = 0.08 μmol) and to search for an alternative labeling position and for an alternative radioisotope respectively. The chemical structure gives less possibility for further nucleophilic attack with [¹⁸F]fluorine, hence we came to the decision to develop an iodinated derivative of sunitinib[®], as the well-established radioisotopes of iodine (¹²³I, ¹²⁴I and ¹²⁵I) could lead to potential useful radiotracers for SPECT and/or PET.

The present paper describes the synthesis of *N*-[2-(diethylamino)ethyl]-5-[(*Z*)-(5-iodo-1,2-dihydro-2-oxo-3*H*-indole-3-ylidene)methyl]-2,4-dimethyl-1*H*-pyrrole-3-carboxamide **4** (5-iodo-sunitinib) and the radiosynthesis of its ¹²⁵I-radiolabeled analogue ¹²⁵I-**4** and reports its preliminary radiopharmacological evaluation.

The nonradioactive compound *N*-[2-(diethylamino)ethyl]-5-[(*Z*)-(5-iodo-1,2-dihydro-2-oxo-3*H*-indole-3-ylidene)methyl]-2,4-dimethyl-1*H*-pyrrole-3-carboxamide **4** (5-iodo-sunitinib) was synthesized for biological evaluation studies and used as reference for the optimization of HPLC elution conditions. The synthetic route proceeded according to a published procedure for the synthesis of sunitinib[®], where a substituted indoline-2-one (oxindole) is reacted with an aldehyde by a Knoevenagel condensation (Scheme 2).¹ The 5-iodo-indoline-2-one **2a**, was prepared by oxidation of commercially available 5-iodoindole **1a** with pyridiniumbromide perbromide (PBPB) in acetic acid following a recently published procedure.¹⁶ The aldehyde, *N*-[2-(diethylamino)ethyl]-2,4-dimethyl-5-formyl-1*H*-pyrrole-3-carboxamide **3**, synthesized as described in the literature¹ was reacted with the starting oxindole **2a** in the presence of piperidine in ethanol affording 5-iodo-sunitinib **4** in 76% yield, a compound that has not been described so far (Scheme 2).

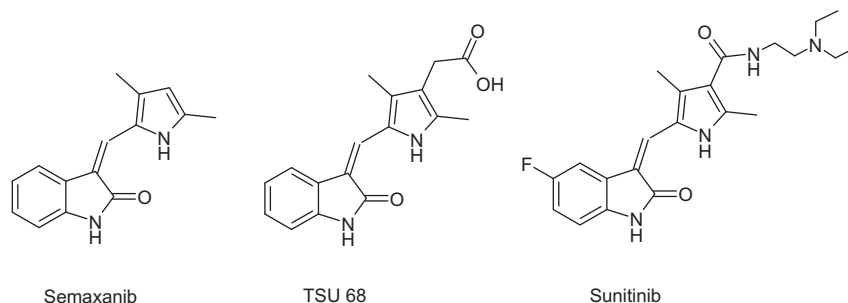
Electrophilic radioiodinations on non-activated aromatic systems are usually performed by means of various demetallation techniques that require organometallic compounds as precursors.

Among the known radioiodo-demetallation reactions, the radioiodo-destannylation is the most favoured method due to the ease of preparation and chemical stability of stannyl precursors.^{17,18}

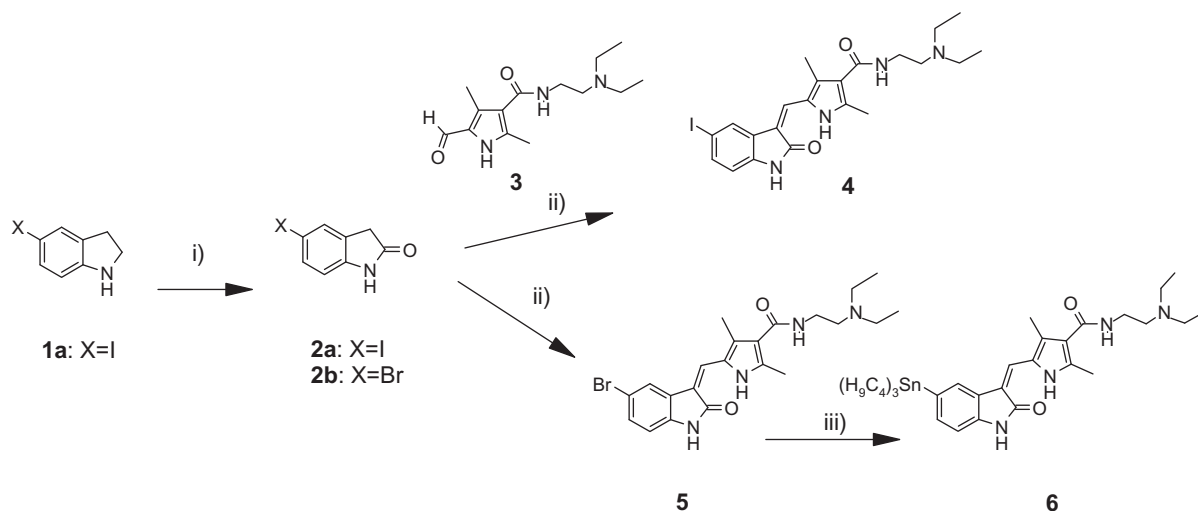
Since stannyl precursors are well established for the radioiodination of various aromatic compounds we investigated the preparation of a trialkylstannyl analogue of 5-iodo-sunitinib. Initially the iodinated compound **4** was treated with hexabutylditin in the presence of catalytic amount of Pd(PPh₃)₂Cl₂. However, in our case the palladium(0) catalyzed cross-coupling reaction did not afford the desired 5-tributylstannylated sunitinib derivative, but a complex mixture of products that was impossible to purify. To overcome this drawback we decided to synthesize an alternative starting compound, 5-bromo-sunitinib **5**, that is available by Knoevenagel condensation of 5-bromoindoline-2-one **2b** with the aldehyde **3** (Scheme 2) and could be obtained in 96% yield. The palladium(0) catalyzed stannylation of the aryl bromide, 5-bromo-sunitinib **5** with hexabutylditin proceeded in dioxan at reflux temperature for 17 h. 5-Tributylstannylated radiolabeling precursor **6** was formed and could be isolated after purification by column chromatography in 41% yield (Scheme 2).

The exocyclic double bond on 3-position of the oxindole as found in molecules of sunitinib type can show an *E/Z* isomerism that is expressed for instance in the appearance of two different signals in the UV-detection of HPLC analysis. This behaviour has already been referred for semaxanib[®] (SU5416), a similar molecule, by Sistla et al. who found that in solid state the compound only exists in the *Z*-configuration, whereas a dissolution and exposure to light results in the formation of an *E*-isomer, which in the dark is converted back to the *Z* isomer.¹⁹ It was documented, that up to 22% *E*-isomer of SU5416 can be formed and that in strong acidic and strong basic HPLC eluent systems the isomerization is suppressed. Similar properties should be expected for sunitinib[®], however we could not find any hint for this in the literature. The first indication was given during setting up a HPLC method for the analytical characterization of 5-iodo-sunitinib **4**, where by the appearance of a second signal the formation of the *E*-isomer of **4** was suspected. This occurred after handling the dissolved compound for some hours at daylight and was unattached by the pH-value of the HPLC eluent in opposite to the findings of Sistla et al. To clarify this phenomenon, anticipating future radiolabeling experiments—since two radiolabeled isomers should be expected as well—we have collected the fractions corresponding to these two peaks in separate vials and investigated them by mass spectrometry. For both fractions the same mass signal of ESI-MS *m/z* = 507.43 (M+H) was found (data not shown).

In addition the isomerization of 5-iodo-sunitinib **4** was confirmed by ¹H NMR experiments; a sample of **4** was dissolved in deuterated DMSO, and the ¹H NMR spectrum was taken from the fresh dissolved solution. The vinyl proton of the *Z*-isomer was detected at 8.22 ppm whereas the aromatic protons of H-4 and H-6



Scheme 1. Structures of the RTK inhibitors based on indoline-2-one.



Scheme 2. Synthesis of 5-iodo-sunitinib **4** and 5-tributylstannylated labeling precursor **6**. Reagents and conditions: (i) PBPB, AcOH/H₂O, 6h, 80 °C; (ii) **3**, EtOH, piperidine, 5 h, 90 °C; (iii) (C₄H₉)₃Sn₂, Pd(PPh₃)₂Cl₂, dioxan, 17 h, reflux.

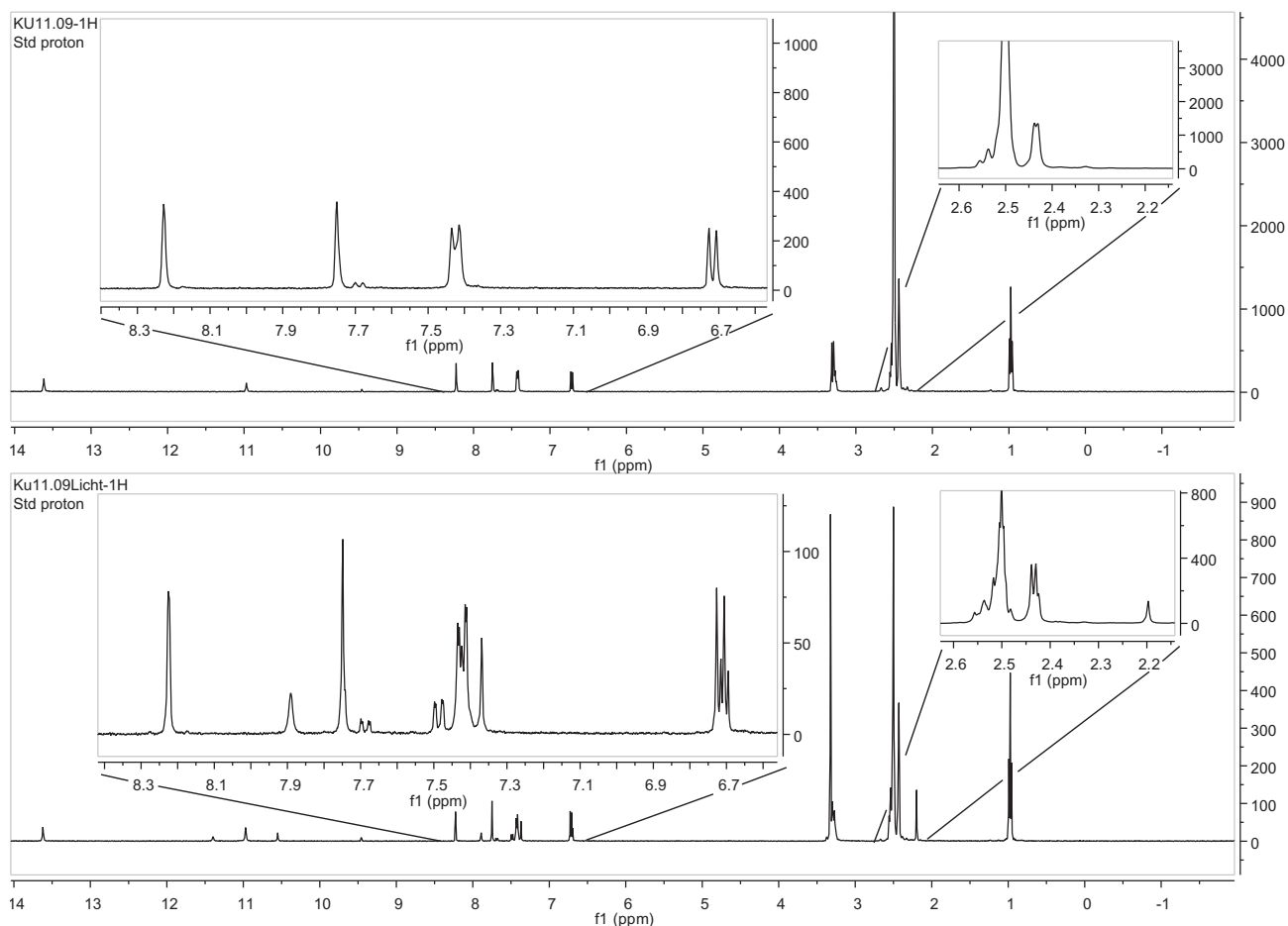


Figure 1. ¹H NMR-spectra of **4** in DMSO-*d*₆ before (upper part) and after exposure of light (lower part)

appeared at 7.41 ppm and 7.42 ppm respectively (Fig. 1, upper part). After exposure to light for 24 hours the ¹H NMR of the same sample was again recorded. In Fig. 1 (lower part) is the appearance of new signals originating from the *E*-isomer demonstrated. So for example at 7.89 ppm the vinyl-proton, at 7.48 ppm the H-6 proton and at 7.36 ppm the H-4 proton of the *E*-isomer of 5-iodo-sunitinib **4** can be found.

Due to the lack of information concerning the inhibitory properties of the new synthesized 5-iodo-sunitinib **4** the compound was submitted to a comprehensive test system for screening compounds against large number of human kinases, KINOMEScan™. This system is based on a competition binding assay that quantitatively measures the ability of a compound to compete with an immobilized, active-site directed ligand. The assay is performed

by combining three components: DNA-tagged kinase; immobilized ligand and the test compound. The ability of the test compound to compete with the immobilized ligand is measured via quantitative PCR of the DNA tag.²⁰

For testing 5-iodo-sunitinib **4** against VEGFR-2 an 11-point 3-fold serial dilution of **4** was prepared in 100% DMSO at 100× final test concentration and subsequently diluted to 1× in the assay (final DMSO concentration = 2.5%). The binding constant (K_d) was calculated from a standard dose-response curve using the Hill equation. Curves were fitted using a non-linear least square fit with the Levenberg-Marquardt algorithm. Fig. 2 displays the curve image for 5-iodo-sunitinib **4**, the amount of kinase measured by qPCR (y-axis) is plotted against the concentration of **4** in nM in log₁₀ scale (x-axis). In a duplicated experimental determination a K_d value of 16 nM for 5-iodo-sunitinib **4** for the inhibition of VEGFR-2 was found. This K_d value is adequately low to justify classification of **4** as an inhibitor of VEGFR-2, as for the lead compound sunitinib a K_i value of 9 nM has been published.²¹

The ability of **4** to inhibit cell proliferation, a mandatory prerequisite for further studies on RTK expressing cells was evaluated by MTT assay in two VEGFR expressing cell lines, primary endothelial HAEC and cancer HT29 cells in comparison with the sunitinib[®]. This assay measures the amount of MTT reduced by a mitochondrial enzyme and assumes that it is proportional to the cell viability. The potency to inhibit cell proliferation was assessed by determination of the IC₅₀, the concentration needed to inhibit cell proliferation by 50%, determined through dose response curves achieved from percentage of cell proliferation plotted against the corresponding compound concentration. IC₅₀ values are presented in Table 1.

These data reflect not only the compound potency to inhibit the tyrosine kinase activity but also its ability to cross the cell membrane. As expected, results indicated that the halogenated compound is able to reduce the cell proliferation demonstrating its ability to both hampering the kinase activity and to penetrate into the cell. Nevertheless the IC₅₀ values analysis in comparison with the parent compound show that its potency as inhibitor is lower than that of sunitinib[®]. These findings, in both cell lines are in agreement with the VEGFR-2 competition binding studies. Even so, the in vitro biological evaluation of the novel compound **4** as VEGFR-2 is promising and prompted us to study its in vivo pharmacokinetics profile.

The radioiodination of the stannylated precursor **6** with [¹²⁵I]NaI was carried out in analogy to a described procedure by Veach et al.²² Using aqueous 30% hydrogen peroxide-acetic acid as the oxidant system, the radioiodinated compound *N*-[2-(diethylamino)ethyl]-5-[(*Z*)-(5-[¹²⁵I]iodo-1,2-dihydro-2-oxo-3*H*-indole-3-ylidene)methyl]-2,4-dimethyl-1*H*-pyrrole-3-carboxamide [¹²⁵I]-**4** was obtained in a radiochemical yield higher than 95% (Scheme 3). [¹²⁵I]-**4** has been purified by RP-HPLC with simultaneous UV and radioactivity detection using a gradient of metha-

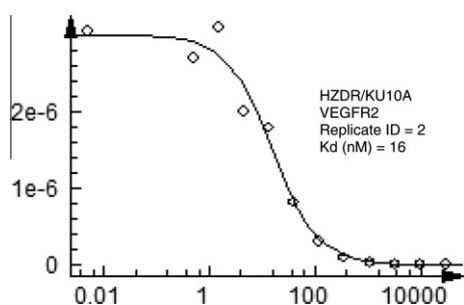


Figure 2. Curve of inhibition of 5-iodo-sunitinib **4** against VEGFR-2, x-axis: amount of VEGFR-2 measured by qPCR, y-axis: concentration of **4** [nM] in log₁₀ scale.

Table 1
Inhibition of cell proliferation

| | Inhibition of cell proliferation IC ₅₀ (μM) | |
|---------------------------|--|-------------|
| | HAEC | HT29 |
| 5-Iodo-sunitinib 4 | 1.12 ± 0.07 | 1.81 ± 0.03 |
| Sunitinib [®] | 0.10 ± 0.07 | 0.33 ± 0.02 |

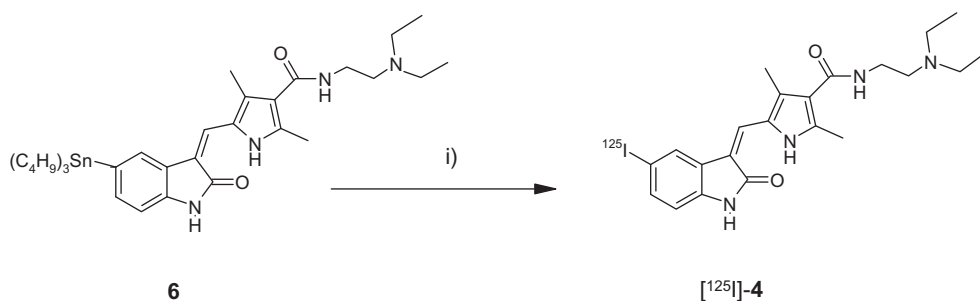
anol/0.1% TFA as eluent (see Supplementary data). The radiochemical purity exceeded 98% as determined by HPLC. The identity of radiolabeled compound [¹²⁵I]-**4** was confirmed by co-elution with reference compound **4**. During the radiolabeling and HPLC purification procedures the exposure of the reactants and the isolated product to light was avoided as far as possible to ensure that the *Z*-isomer of [¹²⁵I]-**4** was the radiochemical species predominantly present and this isomer was used for the following radiopharmaceutical investigation.

Targeting of the intracellular TK domain requires radiotracer penetration into cells. Log D values of 1–3 are considered optimal values to cross the cellular membrane by passive diffusion and reach the target tissue. Low lipophilicity may result in decreased membrane penetration while very high lipophilicity may result in trapping of the drug inside the membrane and increased non-specific binding. In molecular imaging, this type of non-specific binding results in accumulation of radioactivity in the blood pool and low signal/noise ratios in target tissues. The radiolabeled compound [¹²⁵I]-**4** shows an estimated Log D value of 2.25 falling well within the optimal range.

Protein binding affects the tissue distribution and blood clearance of any compound and its uptake by the target organ. The extent of this non-specific binding at various time intervals has been estimated in vitro by incubation of radiolabeled [¹²⁵I]-**4** in fresh human serum at 4 °C and 37 °C (see Supplementary data). Although this method should not be used for an accurate measuring of full protein binding since some disruption of the binding can occur during ethanol precipitation–extraction it can provide an useful prediction of protein binding and also allows to determine the stability in human serum. Data from these studies suggested a low percentage of [¹²⁵I]-**4** bound to the plasmatic proteins (5–10%) indicating a low non-specific binding. By HPLC analysis only the radiolabeled compound was detected in the supernatant, demonstrating its high in vitro stability in human serum. High radiochemical stability of [¹²⁵I]-**4** in saline solution (with 1% Tween-20) was also found up to 24 h when kept in the dark at 37 °C.

Since liver is a major organ of metabolism, samples of mice liver homogenate were incubated with the radiolabeled compound up to 1 h and were analysed by HPLC. In addition to the radiolabeled [¹²⁵I]-**4** (t_r = 22.7 min) a more polar radiolabeled compound (t_r = 11.3 min) was detected in the HPLC radiochromatogram (data not shown). This probably corresponds to the *N*-desethyl metabolite as metabolism studies with the analogous inactive fluorinated compound sunitinib[®], have revealed. It was found that metabolism of sunitinib by liver enzymes, particularly CYP3A4, results in the formation of *N*-desethyl-sunitinib (SU12662) a still active metabolite, by desalkylation of the basic chain.²³

Preliminary biodistribution studies of [¹²⁵I]-**4** were carried out in healthy CD-1 female mice at 1 h and 4 h after administration (a.a.) to evaluate the preferential uptake and clearance in most relevant organs. Data from these studies expressed as the percentage of injected dose per g organ is shown in Figure 3, indicating a rapid clearance from most organs including blood and a relative high in vivo stability. A relatively high uptake in VEGFR-2 rich tissues (kidney and lung) was observed. The total urinary radioactivity was excreted as a radiochemical species with the same retention time as free radioiodine as demonstrated by HPLC analysis of



Scheme 3. Radiosynthesis of 5-[¹²⁵I]iodo-sunitinib ([¹²⁵I]-4). Reagents and conditions: (i) [¹²⁵I]NaI, MeOH, H₂O₂/AcOH, 10 min, rt.

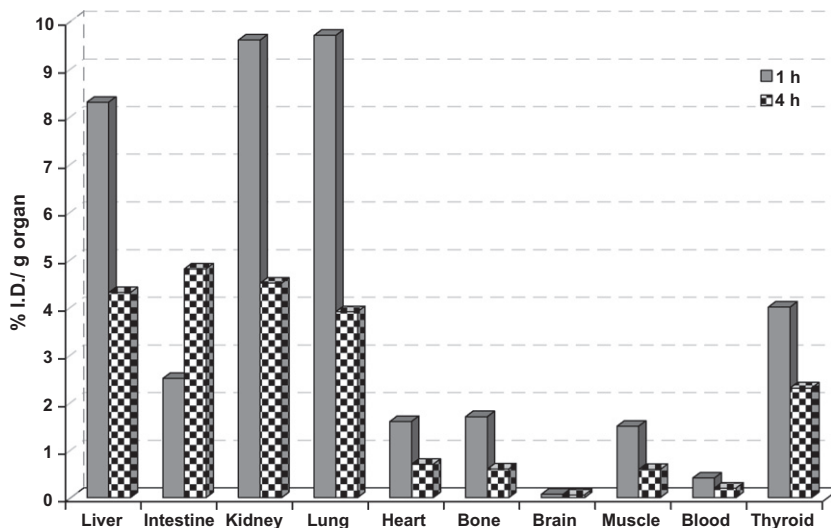


Figure 3. Biodistribution data in most relevant organs, expressed as % ID/g organ for 5-[¹²⁵I]iodo-sunitinib([¹²⁵I]-4) at 1 and 4 h after IP administration in healthy CD-1 female mice.

samples collected at sacrifice time, revealing some *in vivo* deiodination. On the other hand, the *in vivo* instability of radioiodinated compounds is commonly reflected by a high amount of radioactivity accumulation in the thyroid, however the low thyroid levels found (4 and 2.3%ID/g at 1 and 4 h respectively) indicate that the compound is relatively stable *in vivo* up to 4 h.

The search for radiotracers towards VEGFR expression and for monitoring *in vivo* processes involved with tumor proliferation and angiogenesis, suggested us the development of a radiolabeled derivative of sunitinib[®]. We focused on the labeling with radioiodine, because the number of its radioisotopes available for the clinic (¹²³I, ¹²⁴I and ¹²⁵I) could offer the utilization as potential radiotracer for SPECT and PET as well. Additionally application of latest ¹⁸F labeling techniques like [¹⁸F]Selectfluor bis(triflate)²⁴ to the stannylated precursor **6** or utilization of a palladium-based electrophilic fluorination reagent as published recently by Lee et al.²⁵ could give access to an isotopic ¹⁸F-labeled sunitinib[®].

The novel 5-iodo-sunitinib **4** was synthesized and identified as VEGFR-2 inhibitor having a *K_d* value of 16 nM. The corresponding radiolabeled analogue 5-[¹²⁵I]iodo-sunitinib [¹²⁵I]-**4** was obtained in high radiochemical yield (>95%) and radiochemical purity (>98%). Lipophilicity of [¹²⁵I]-**4** was found to be 2.25. Determination of human plasma protein binding suggested a low non-specific binding of 5–10%. Biodistribution studies in healthy mice showed a relatively high uptake of [¹²⁵I]-**4** in VEGFR-2 rich tissue like kidney and lung, its high stability in human serum and urine samples suggests that the tracer is not significantly metabolized. In summary these preliminary pharmacological data suggest that a radiiodin-

ated sunitinib may act as promising radiotracer for imaging angiogenic processes and the results encourage further radiolabeling experiments with the PET radioisotope ¹²⁴I for *in vivo* imaging of VEGFR expressing tumours.

Acknowledgments

The authors want to thank Dr. Lars Ruddigkeit, Department of Chemistry and Biochemistry at the University of Bern (Switzerland) for helpful discussions.

This work was financially supported by DAAD (Germany) and FCT (Portugal) by the Acções Integradas/DAAD-GRICES, project number 0811983.

Supplementary data

Supplementary data associated with this article can be found, in the online version, at doi:10.1016/j.bmcl.2012.02.068.

References and notes

- Sun, L.; Liang, C.; Shirazian, S.; Zhou, Y.; Miller, T.; Cui, J.; Fukuda, J. Y.; Chu, J. Y.; Nematalla, A.; Wang, X.; Chen, H.; Sistla, A.; Luu, T. C.; Tang, F.; Wei, J.; Tang, C. *J. Med. Chem.* **2003**, *46*, 1116.
- Haubner, R.; Wester, H. J.; Weber, W. A.; Schwaiger, M. *Quart J. Nucl. Med.* **2003**, *47*, 189.
- Haubner, R.; Wester, H. J. *Curr. Pharm. Des.* **2004**, *10*, 1439.
- Choe, Y. S.; Lee, K. H. *Curr. Pharm. Des.* **2007**, *13*, 17.
- Hicks, J. W.; VanBrocklin, H. F.; Wilson, A. A.; Sylvain, H.; Vasdev, N. *Molecules* **2010**, *15*, 8260.

6. Samen, E.; Thorell, J.-O.; Lu, L.; Tegnebratt, T.; Holmgren, L.; Stone-Elander, S. *Eur. J. Nucl. Med. Mol. Imaging* **2009**, *36*, 1283.
7. Ilovich, O.; Billauer, H.; Dotan, S.; Mishani, E. *Bioorg. Med. Chem.* **2010**, *18*, 612.
8. Ilovich, O.; Jacobson, O.; Aviv, A.; Litchi, R.; Chisin, R.; Mishani, E. *Bioorg. Med. Chem.* **2008**, *16*, 4242.
9. Ilovich, O.; Aberg, O.; Langström, B.; Mishani, E. *J. Label. Compds. Radiopharm.* **2009**, *52*, 151.
10. Mishani, E.; Abourbeh, G. *Curr. Top. Med. Chem.* **2007**, *7*, 1755.
11. Mishani, E.; Abourbeh, G.; Eiblmaier, M.; Anderson, C. J. *Curr. Pharm. Des.* **2008**, *14*, 2983.
12. Mishani, E.; Hagooley, A. J. *Nucl. Med.* **2009**, *50*, 1199.
13. Gelovani, J. G. *Cancer Metastasis Rev.* **2008**, *27*, 645.
14. Wang, J. Q.; Miller, K. D.; Sledge, G. W.; Zheng, Q. H. *Bioorg. Med. Chem. Lett.* **2005**, *15*, 4380.
15. Kniess, T.; Bergmann, R.; Kuchar, M.; Steinbach, J.; Wuest, F. *Bioorg. Med. Chem.* **2009**, *17*, 7732.
16. Bouchiki, F.; Anizon, F.; Moreau, P. *Eur. J. Med. Chem.* **2008**, *43*, 755.
17. SeEVERS, R. H.; Counsell, R. E. *Chem. Rev.* **1982**, *82*, 575.
18. Kabalka, G. W.; Varma, R. S. *Tetrahedron* **1989**, *45*, 6601.
19. Sistla, A.; Yang, W. L.; Shenoy, N. *J. Chromatogr. A* **2006**, *1110*, 73.
20. Fabian, M. A.; Biggs, W. H.; Treiber, D. K.; Atteridge, C. E.; Azimioara, M. D.; Benedetti, M. G.; Carter, T. A.; Cireci, P.; Edeen, P. T.; Floyd, M.; Ford, J. M.; Galvin, M.; Gerlach, J. L.; Grotzfeld, R. M.; Herrgard, S.; Insko, D. E.; Insko, M. A.; Lai, A. G.; Lelias, J. M.; Metha, S. A.; Milanov, Z. V.; Velasco, A. M.; Wodicka, L. M.; Patel, H. K.; Zarrinkar, P. P.; Lockhart, D. J. *Nat. Biotechnol.* **2005**, *23*, 329.
21. Mendel, D. B.; Laird, D. A.; Xin, X.; Louie, S. G.; Christensen, J. G.; Li, G.; Schreck, R. E.; Abrams, T. J.; Ngali, T. J.; Lee, L. B.; Murray, L. J.; Carver, J.; Chan, E.; Moss, K. G.; Haznedar, J. Ö.; Sukbuntherng, J.; Blake, R. A.; Sun, L.; Tang, C.; Miller, T.; Shirazian, S.; McMahon, G.; Cherrington, J. M. *Clin. Cancer Res.* **2003**, *9*, 327.
22. Veach, D. R.; Namavari, M.; Beresten, T.; Balatoni, J.; Minchenko, M.; Djaballah, H.; Finn, R. D.; Clarkson, B.; Gelovani, J. G.; Bornmann, W. G.; Larson, S. M. *Nucl. Med. Biol.* **2005**, *32*, 313.
23. Buckstein, R.; Meyer, R. M.; Seymour, L.; Biagi, J.; Mackay, H.; Laurie, S.; Eisenhauer, E. *Curr. Oncol.* **2007**, *14*, 154.
24. Teare, H.; Robins, E. G.; Kirjavainen, A.; Forsback, S.; Sandford, G.; Solin, O.; Luthra, S. K.; Gouverneur, V. *Angew. Chem.* **2010**, *122*, 6973.
25. Lee, E.; Kamlet, A. S.; Powers, D. C.; Neumann, C. N.; Boursalian, G. B.; Furuya, T.; Choi, D. C.; Hooker, J. M.; Ritter, T. *Science* **2011**, *334*, 639.